Asian Journal of Atmospheric Environment
Vol. 7-2, pp.95-104, June 2013
doi: http://dx.doi.org/10.5572/ajae.2013.7.2.095

Thermal Distribution of Size-resolved Carbonaceous Aerosols and Water Soluble Organic Carbon in Emissions from Biomass Burning

Min-Suk Bae* and Seung-Shik Park[1)]

Department of Environmental Engineering, Mokpo National University, Muan-gun, Jeonnam 534-729, Korea
[1)]Department of Environmental Engineering, Chonnam National University, Gwangju 500-757, Korea

*Corresponding author. Tel: +82-61-450-2485, E-mail: minsbae@hotmail.com

ABSTRACT

The study of carbonaceous aerosols in the atmosphere is critical to understand the role of aerosols in human health and climate. Using standardized thermal optical transmittance methods, organic carbon (OC), elemental carbon (EC), and water soluble organic carbon (WSOC) were determined using a combustion sampling system for four types of agricultural crop residues (rice straw, red pepper stems, soybean stems, and green perilla stems) and eight types of forest trees (pine stems, pine needles, ginkgo stems, ginkgo leaves, maple stems, maple leaves, cherry stems, and cherry leaves). The aerosol particles between 0.056 and 5.6 μm in size were analyzed using a Micro-Orifice Uniform Deposit Impactor (MOUDI). In the current study, the Carbonaceous Thermal Distribution (CTD) by carbon analyzer was discussed in order to understand the carbon fractions from the twelve types of biomass burning. Also, the concentration of OC, EC, WSOC, and water insoluble organic carbon (WIOC) detected in the emissions were described.

Key words: Carbonaceous Thermal Distribution, Organic Carbon, Biomass Burning, Source

1. BACKGROUND

Although ambient aerosols include large amounts of organic compounds, every organic molecular structure in these aerosols is not yet completely identified. These organic compounds can scatter or absorb incoming solar radiation, resulting in a change in the albedo of the earth and impairment in visibility (Thompson *et al.*, 2012; Park *et al.*, 2010). The toxic effects of atmospheric organic compounds depend on the inherent toxicity of the compound and its lifetime in the atmosphere (Baddock *et al.*, 2013). Carbonaceous aerosols can be classified as organic carbon (OC) and elemental carbon (EC), the main components of aerosols in the atmosphere (Schneidemesser *et al.*, 2010; Bae *et al.*, 2004). Sources of carbonaceous aerosols include stationary and mobile combustion sources, biological sources, and the oxidation of anthropogenic and natural gaseous organic species that form reaction products that condense to form secondary organic aerosols (SOAs). The complex chemistry of organic aerosols and the associated precursors for SOA formation present major challenges for measurement, modeling, and development of control strategy to mitigate carbonaceous aerosols (Vivanco *et al.*, 2011).

The composition of the organic compounds in atmospheric aerosols has been studied for several decades. Although years of effort have been expended in the application of the most sophisticated equipment and techniques including mass spectrometric techniques such as gas chromatography, less than 40% of the total mass ratio of the particulate organic matter has been characterized (Bae *et al.*, 2012; Miller-Schulze *et al.*, 2011). Among many techniques, collection of aerosols on quartz fiber filters is widely used for laboratory-based chemical analyses. An important measurement of carbonaceous aerosol is the thermal-optical measurement of OC and EC, which are measured by heating a portion of the quartz fiber filter to progressively higher temperatures, oxidizing the evolved gases to carbon dioxide and then analyzing the carbon dioxide with a nondispersive infrared sensor (NDIR) or flame ionization detector (FID) (Chow *et al.*, 2007; Birch, 1998). The method of OC and EC analysis can determine concentrations, which can be used to estimate potential sources using a source apportionment model and to characterize the behavior of atmospheric carbon by providing a method for identifying secondary organic carbon (Zhang *et al.*, 2009).

Based on the analytical approach of applying the

thermal-optical technique for OC and EC, different simplified analytical carbon fractions such as OC1, OC2, OC3, OC4, Pyrolyzed Carbon (PC), and EC have been widely used for understanding the carbon fractions in carbonaceous aerosols. These carbon fractions can be defined by certain time steps related to the analysis temperature of the pre-programmed OC/EC instrument setting. OC1 is the most volatile of the four OC fractions, and OC4 is the least volatile of the four OC fractions. Therefore, several researchers have investigated the thermal analytical method for carbonaceous aerosols, and they have discovered that the CTD obtained from converted carbon dioxide showed a different evolution depending on the sources and chemical composition of the carbon. Novakov and Corrigan (1996) reported the CTD for cloud condensation nucleus activity from biomass smoke, and Peralta *et al*. (2007) presented the CTD of aromatic compounds with a varying number of aromatic rings.

OC consists of water-soluble and water-insoluble organic carbon (WSOC and WIOC) compounds. WSOC compounds account for a large fraction of the OC mass in many locations (Pathak *et al*., 2011). The WSOC compounds have both primary and secondary sources that can be biogenic or anthropogenic. Biomass burning is another important source of WSOC (Sullivan and Weber, 2006). WSOC has potential as a tracer for biomass burning plumes and the SOAs, where WSOC may play an important role. The hydrophilic WSOC fraction is typically composed of highly oxygenated compounds with low molecular weights including aliphatic carboxylic acids and carbonyls, saccharides, and amines. The hydrophobic WSOC is composed of compounds with high molecular weights such as aliphatic carboxylic acids and carbonyls, aromatic acids, phenols, organic nitrates, cyclic acids, and Suwannee River fulvic acids.

The types of biomass that were burned are comprised of soft woods, hard woods, and grasses from temperate, tropical and arctic climate areas, with cellulose as a reference material. Although levoglucosan is the key molecular marker related to the biomass, burning sources have been investigated in many studies (Bae *et al*., 2012). Few investigators have studied size resolution in biomass combustion related to carbonaceous aerosols. Biomass organic markers can be formed as a product from the thermal breakdown of cellulose during the burning processes and can be used as organic tracer compounds. In the United States, wood smoke from fireplaces is one of the major sources. Levoglucosan is a molecular marker for biomass burning, where polycyclic aromatic hydrocarbons (PAHs), aldehydes, and free radicals are formed. Those chemicals are very toxic or mutagenic. Several studies have reported an association between wood smoke exposure and adverse health effects, including eye, nose, and throat irritation, decrements in lung function, and increased respiratory infections (Smith, 2000). The biomass burning emissions are certainly different in the USA. One of the major contributors is the vegetation burning in the fall season after harvest, which contains primarily biopolymers with minor amounts of lipids and terpenoids. The other contributor is wildfire in all seasons except the rainy period in the summertime. Unfortunately, little information is available from analyses performed in Korea due to the limitations of available analytical techniques for carbon measurement and/or analysis.

The purpose of this study is to report the concentrations of carbonaceous aerosols detected in the emissions from four types of agricultural crop residues (rice straw, red pepper stems, soybean stems, and green perilla stems) and eight types of forest trees (pine stems, pine needles, ginkgo stems, ginkgo leaves, maple stems, maple leaves, cherry stems, and cherry leaves) in aerosols with particles between 0.056 and 5.6 μm in size. Concentrations of OC, EC, WSOC, and WIOC are described.

2. METHODS

2.1 Sampling of Particulate Matter Emissions from Biomass Burning

A total of 12 biomass materials were combusted to examine the characteristics of the aerosol emissions and the size distributions of the chemical components. The detailed description of sampling method can be found elsewhere (Park *et al*., 2013). Briefly, the target materials burned included four agricultural crop residues (rice straw, soybean stems, green perilla stems, and red pepper stems) and eight types of forest tree (pine needles, pine stems, cherry leaves, cherry stems, maple leaves, maple stems, ginkgo stems, and ginkgo leaves). The crop residues and forest trees were collected from rural fields. A schematic diagram of the combustion sampling system is presented in Fig. 1. The sampling system includes a combustion pan, hood, clean background air injection component, dilution tunnel, and MOUDI in a laboratory hood. The biomass materials were ignited with a butane torch in the stove to make biomass smoke. Biomass combustion emissions were collected using a Micro-Orifice Uniform Deposit Impactor (MOUDI 110, MSP corp., Shoreview, MN, USA) with a sampling flow rate of 30 liters per minute (L/min) between 0.056 and 5.6 μm aerosol size. During the combustion experiments, one set of MOUDI samples for each biomass type

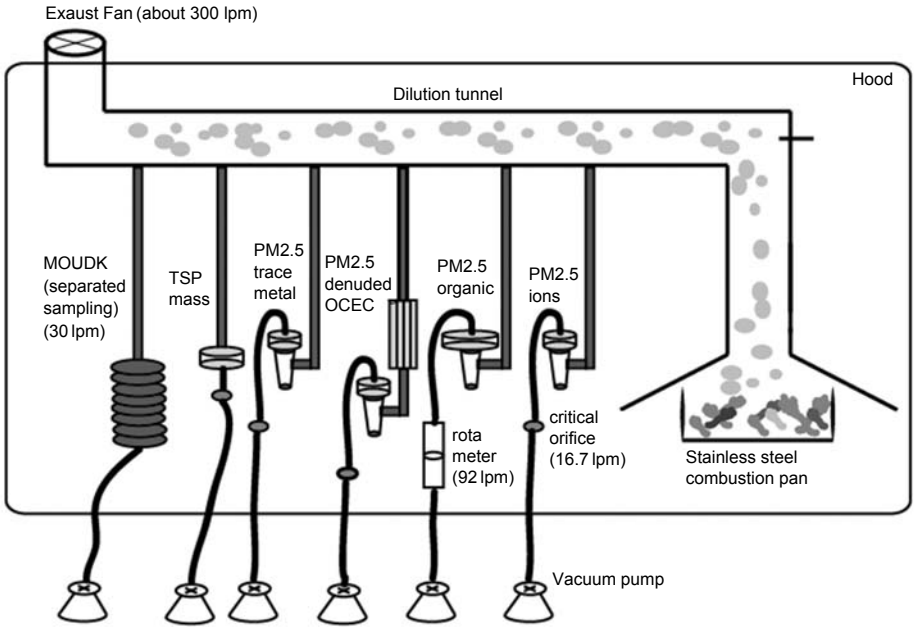

Fig. 1. A schematic diagram of the combustion sampling system.

Table 1. Description of aerosol emission factors for OC, EC, WSOC, and WIOC.

Type of biomass	Sampling time (s)	Combustion rate (g/s)	Combustion mass (g)	OC (g/kg)	EC (g/kg)	WSOC (g/kg)	WIOC[1] (g/kg)	WSOC/OC
Agricultural crop residues								
Rice straw	30	0.20	5.96	6.62	0.40	1.72	4.90	0.26
Red pepper stem	40	0.22	8.72	4.01	0.82	2.29	1.72	0.57
Soybean stem	40	0.25	9.91	0.94	4.16	0.46	0.48	0.49
Green perilla stem	40	0.30	11.81	1.58	1.33	0.76	0.82	0.48
Forest tree types								
Pine stem	40	0.17	6.72	2.86	1.23	1.49	1.38	0.52
Pine needles	40	0.16	6.36	8.20	0.42	1.72	6.48	0.21
Ginkgo stem	40	0.14	5.74	2.26	1.20	0.54	1.72	0.24
Ginkgo leaves	35	0.23	8.05	3.24	1.06	0.49	2.75	0.15
Maple stem	40	0.12	4.85	14.32	0.29	7.45	6.88	0.52
Maple leaves	40	0.26	10.44	1.39	1.13	0.53	0.86	0.38
Cherry stem	40	0.12	4.77	9.16	0.95	4.67	4.49	0.51
Cherry leaves	40	0.40	15.88	0.49	0.89	0.14	0.35	0.29

[1]WIOC=differences between OC and WSOC

were collected on quartz substrates with backup Teflon filters. Size-resolved measurements of PM emitted during biomass burning were strictly limited to 40-60 seconds to prevent nozzle blockage in the lower stages (Table 1). The OC, EC, WSOC, and calculated WIOC (difference between OC and WSOC) concentrations were determined from the MOUDI samples. Blank values were subtracted from measured concentrations for each impactor stage.

2.2 OC/EC Analysis

The CTD analysis was performed using standardized OC and EC measurements obtained with a semi-continuous OC/EC carbon aerosol analyzer (Sunset Laboratory, Inc., Hillsborough, NC, USA) Using the thermal-optical transmittance (TOT) method (Birch, 1998; Birch and Cary, 1996), the MOUDI samples were collected onto pre-baked and pre-weighed 47-mm quartz substrates. After collecting the aerosol, the filter was heated through a series of temperature steps

that follow the NIOSH protocol (Birch and Cary, 1996). The analytical procedure is comprised of three parts. In the first part, the loaded filter is heated to 840°C in the presence of pure (oxygen-free) helium gas, and organic compounds and pyrolysis products are thermally released from the aerosol on the filter. Desorbed carbon fragments are oxidized to CO_2 using MnO_2 as a catalyst, then converted to CH_4 for FID detection. EC is also detected in a similar way at the second stage, but the maximum temperature is 870°C and the analysis is performed under a He/O_2 atmosphere. During the last stage, a fixed volume of methane is analyzed as an internal standard for quantification. During the entire analysis, laser transmittance is used to determine the split between OC and EC by correcting for the EC formed during the first stage of the analysis in the helium atmosphere. To validate the accuracy of the OC/EC analyzer, external calibration has been checked with five different injections at different concentrations. The average of the recoveries was 0.98 ± 0.02, and the calibration check had a correlation factor of 0.999. The instrument blank test, which was conducted after completing the analysis, was conducted several times to assess the noise and contamination by the instrument and filter.

2.3 WSOC Analysis

The collected quartz fiber and Teflon filter samples for each biomass type were extracted with 25 mL of ultra high-purity water (Barnstead Nanopure, #D11901, Thermo Scientific, USA) via ultrasonication for 60 minutes at room temperature. The water extracts were filtered using a syringe membrane filter (Millipore 0.45 μm) to remove insoluble particles. Extracts were then analyzed for eight ionic species and oxalate, as well as WSOC, using ion chromatography (IC, Metrohm861), and a total organic carbon analyzer (TOC, Sievers 5310C, USA). The detailed discussions for ion concentrations can be found elsewhere (Park *et al*., 2013). We only described the result of WSOC by TOC in this study.

Briefly, in the TOC analyzer, the organic compounds dissolved in ultrapure water were oxidized to form carbon dioxide using an ultraviolet (UV) lamp and ammonium persulfate as a chemical oxidizing agent. The CO_2 formed was then measured using a membrane-based conductivity detection technique. The total carbon (TC) and inorganic carbon (IC) standard solutions were prepared with reagent grade potassium hydrogen phthalate ($KHC_8H_4O_4$) and sodium carbonate (Na_2CO_3) to calibrate the instrument. TOC concentration was calculated as the difference between TC and IC. The average blank values and standard deviation of blanks were 0.10 and 0.004 μgC mL^{-1}. The calculated MDL was 0.11 μgC mL^{-1}. Sample precision was 5.6%.

3. RESULTS AND DISCUSSION

Table 1 shows the aerosol emission factors for OC, EC, WSOC, and WIOC emitted from the combustion of agricultural crop residues and forest tree types that were measured using MOUDI. MOUDI results were constructed by summing results from each stage of the impactor to yield integrated OC, EC, WSOC, and WIOC concentrations. A dilution factor of 250 was applied for the aerosol emission factor values. Concentrations of OC span the most abundant from 0.94 (soybean stems) to 14.32 (maple stems) (g compound per kg biomass). The relative trends for all biomass concentrations were measured with MOUDI. In a previous study, Schauer *et al*. (2001) reported the emission rates for the combustion of three types of wood. The emission rates were 9.5 ± 1.0, 5.1 ± 0.5, and 8.5 ± 0.8 g kg^{-1} of pine, oak, and eucalyptus burned. *n*-Butane and *n*-heptane emissions are smaller but still significantly larger than the emissions of any of the remaining alkanes. In another study, Kleeman *et al*. (2008) presented the emission rates of 6.55, 3.03, 4.59, and 3.91 g kg^{-1} for combustion of pine, oak, eucalyptus, and rice straw, respectively. In the current study, we found emission rates of 6.62, 4.01, 0.94, and 1.58 for rice straw, red pepper stems, soybean stems, and green perilla stems, respectively. Eight types of the forest trees yield emission factors of 2.86, 8.20, 2.26, 3.24, 14.32, 1.39, 9.16, and 0.49 for pine stems, pine needles, ginkgo stems, ginkgo leaves, maple stems, maple leaves, cherry stems, and cherry leaves, respectively. The averaged emission factor for the agricultural crop residues is approximately 37% lower than the averaged emission factor for the forest tree types. Table 1 also presets WSOC/OC ratios, which lie between 0.15 (ginkgo leaves) and 0.57 (red pepper stems).

3.1 Rice Straw, Red Pepper Stems, Soybean Stems, and Green Perilla Stems

Fig. 2 illustrates the sized resolved CTD (top), size distribution of WIOC, WSOC, and EC with a size distribution ratio of OC to EC associated with rice straw, red pepper stems, soybean stems, and green perilla stems. The CTD shows that the thermal evolution of carbonaceous aerosols is different than during instrumental analysis. The CH_4 value detected from FID can be used to calculate the carbon concentration. The CTD can have different patterns that are related to their origins and/or chemical structures under the

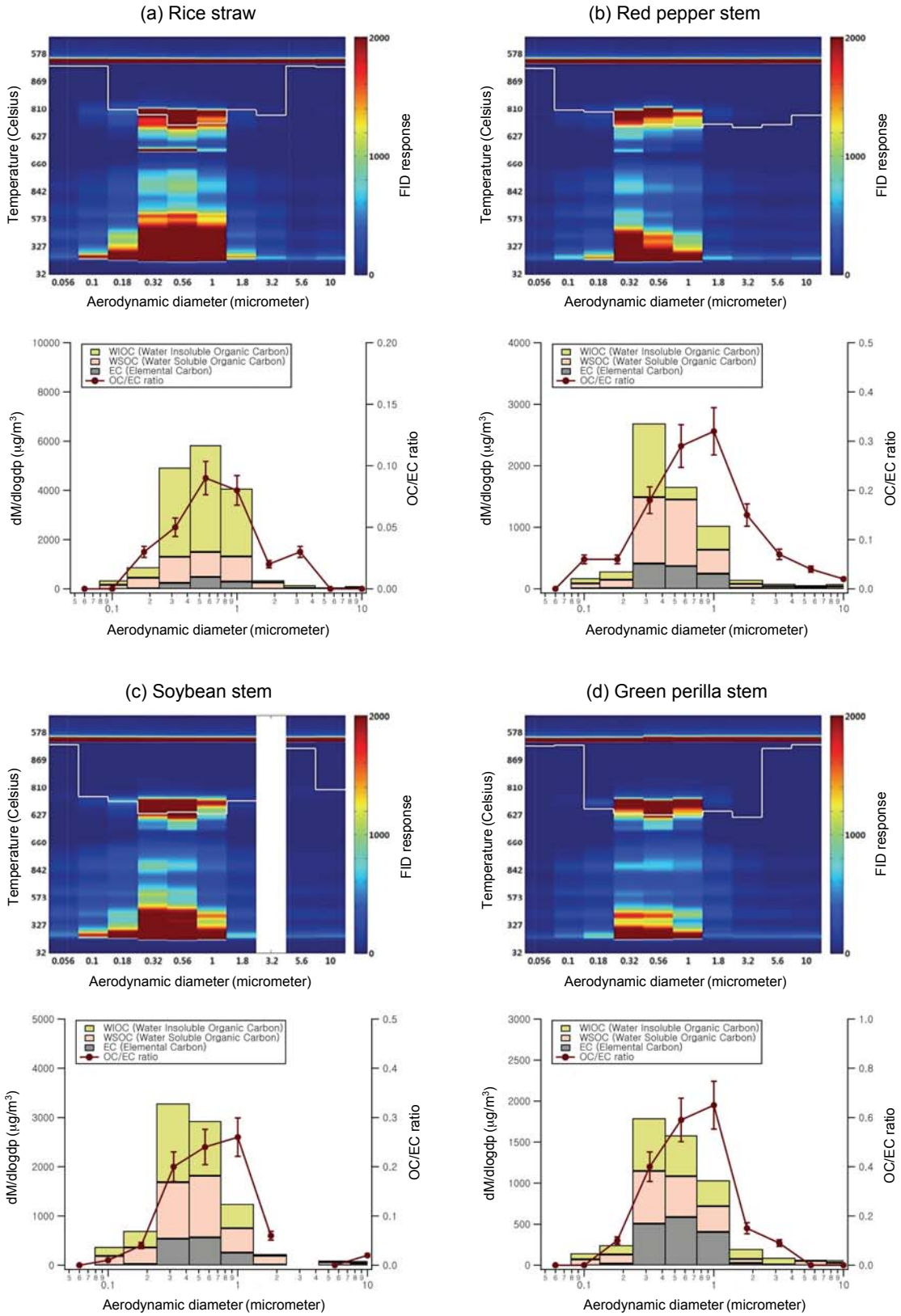

Fig. 2. Sized resolved CTD (top), size distribution of WIOC, WSOC, EC, and OC/EC ratio (bottom) associated with (a) rice straw, (b) red pepper stem, (c) soybean stem, and (d) green perilla stem.

NIOSH temperature protocol. In this study, the CH_4 peaks and the temperature protocol over the entire size range were determined simultaneously by using the graphical CTD while analyzing the actual temperature and CH_4 levels as shown in Fig. 2. These results can be provided in one plane as a contour plot. The contour plot of the CTD in Fig. 2(a) shows the CH_4 concentrations in each bin (in dCH_4 ppm/dt) with baseline corrections. The vertical axis is the analysis temperature (°C), and the horizontal axis is the size (μm). The CTD analysis can provide two important points of information: (1) the identification of detailed analytical carbon evolution peaks that are related to temperature by understanding the split time variations for the OC and EC analytical concentrations; and (2) the characterization of the separated sizes that are related to the carbon evolution.

The CTD patterns for the rice straw, red pepper stems, soybean stems, and green perilla stems is shown in Fig. 2. Novakov and Corrigan (1996) provided the CTD for the nucleation of cloud condensation from biomass smoke. Peralta *et al*. (2007) presented the CTD of aromatic compounds, which varied with the number of aromatic rings. This study can give information about the organic structure such as the PAHs related to biomass burning if the amount of evolved carbon exists at the higher temperature. Similar peaks are observed in the CTD patterns for red pepper stems, soybean stems, and green perilla stems, but not for rice straw. The peak increases to 0.32 μm size while the rice straw shows a 0.56 μm size. The cause of this peak may be inferred from the emissions of the different organic molecular marker compounds related to primary combustion. However, all of the agricultural crop residues indicate the CTD at the lower temperature. This result suggests that the functional groups of organic compounds from agricultural crop residues could be similar.

Rice straw sources have total particulate carbon size distributions that peak at 0.56 μm size, while red pepper stem, soybean stem, and green perilla stem carbon aerosols peak at a size of 0.32 μm. Source apportionment studies often use either the OC/EC or EC/OC ratio as a chemical signature to identify source contributions. OC/EC with size distributions are good candidates for simple tracers that can be used for size-resolved source apportionment studies. Similarities between size distributions can be judged by calculating the correlation coefficient (R^2) between ratios of two species, treating each size fraction as a different observation. WIOC concentrations had unimodal size distributions that were highly correlated (R^2 of 0.96) with OC concentrations compared to R^2 of 0.75 between WSOC and OC, suggesting that the resolution of source apportionment studies for airborne particulate matter is greatly increased by the use of unique organic tracers that are released only by a well-defined class of sources. Each biomass size distribution pattern in the agricultural crop residues was well correlated between OC and WIOC size distributions, suggesting that organic compounds in WIOC could serve as an appropriate tracer for agricultural crop residue contributions to ultrafine aerosol concentrations. However, we need to consider that levoglucosan as a WSOC was the most abundant organic compound measured in the $PM_{1.8}$ size fraction of wood and rice straw (Kleeman *et al*., 2008). Levoglucosan size distributions measured in the previous study were not highly correlated with EC and OC size distributions from all biomass combustion sources because a significant number of levoglucosan measurements were missing due to corrupted data files discovered during the final phase of quantification. Additional data analysis was performed to determine if levoglucosan concentrations that are available suggest any enhancement or reduction in levoglucosan concentrations as a function of size. For the agricultural crop residues, we need to develop the ratios of WIOC compounds to levoglucosan to determine detailed source identification in Korea.

3.2 Pine Stems, Pine Needles, Ginkgo Stems, and Ginkgo Leaves

Fig. 3 illustrates the size-resolved CTD (top), size distribution of WIOC, WSOC, and EC with a size distribution ratio of OC to EC associated with pine stem, pine needles, ginkgo stem, and ginkgo leaves. The CTD size patterns for pine stems, pine needles, ginkgo stems, and ginkgo leaves shown in Fig. 3 can be divided into two patterns. One is a stem pattern (pine and ginkgo stems), and the other is a leaf pattern (pine needle and ginkgo leaves). The peak in the stem pattern increases to 0.32 μm size, while leaf patterns have a 1.0 μm size. The cause of the two different patterns could also be related to the emissions of the different organic molecular markers associated with stems and leaves in biomass burning. The CTD for both ginkgo stems and ginkgo leaves is present at the high temperature (>800°C) in He during OC analysis by carbon analyzer. This observation shows that aromatic compounds, which have a higher number of aromatic rings, might be related to ginkgo tree combustion.

Each biomass size distribution pattern is well correlated between OC and WIOC size distributions (R^2 of 0.98), also suggesting that organic compounds in WIOC can serve as an appropriate tracer for pine and ginkgo tree type contributions to ultrafine aerosol

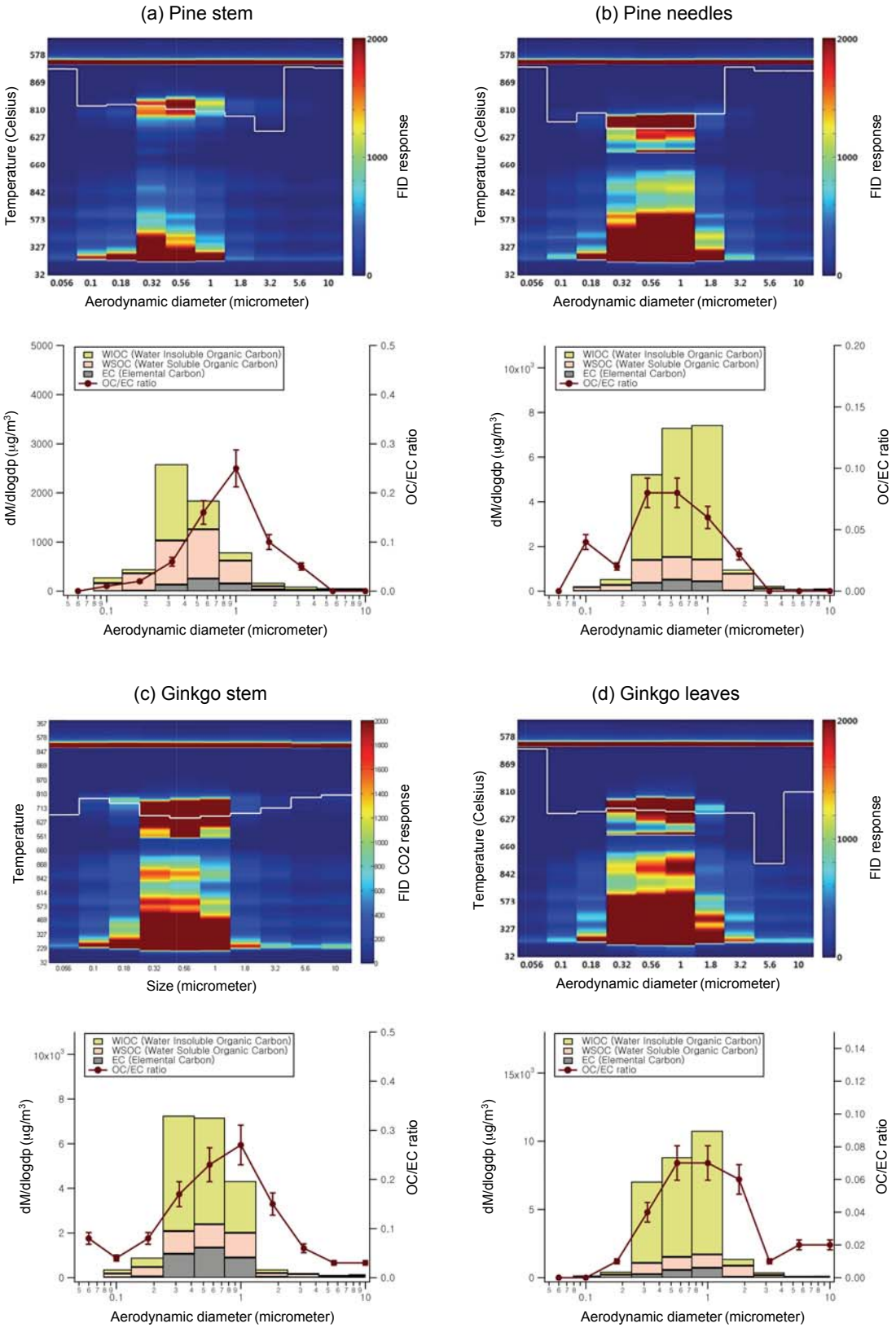

Fig. 3. Sized resolved CTD (top), size distribution of WIOC, WSOC, EC, and OC/EC ratio (bottom) associated with (a) pine stem, (b) pine needles, (c) ginkgo stem, and (d) ginkgo leaves.

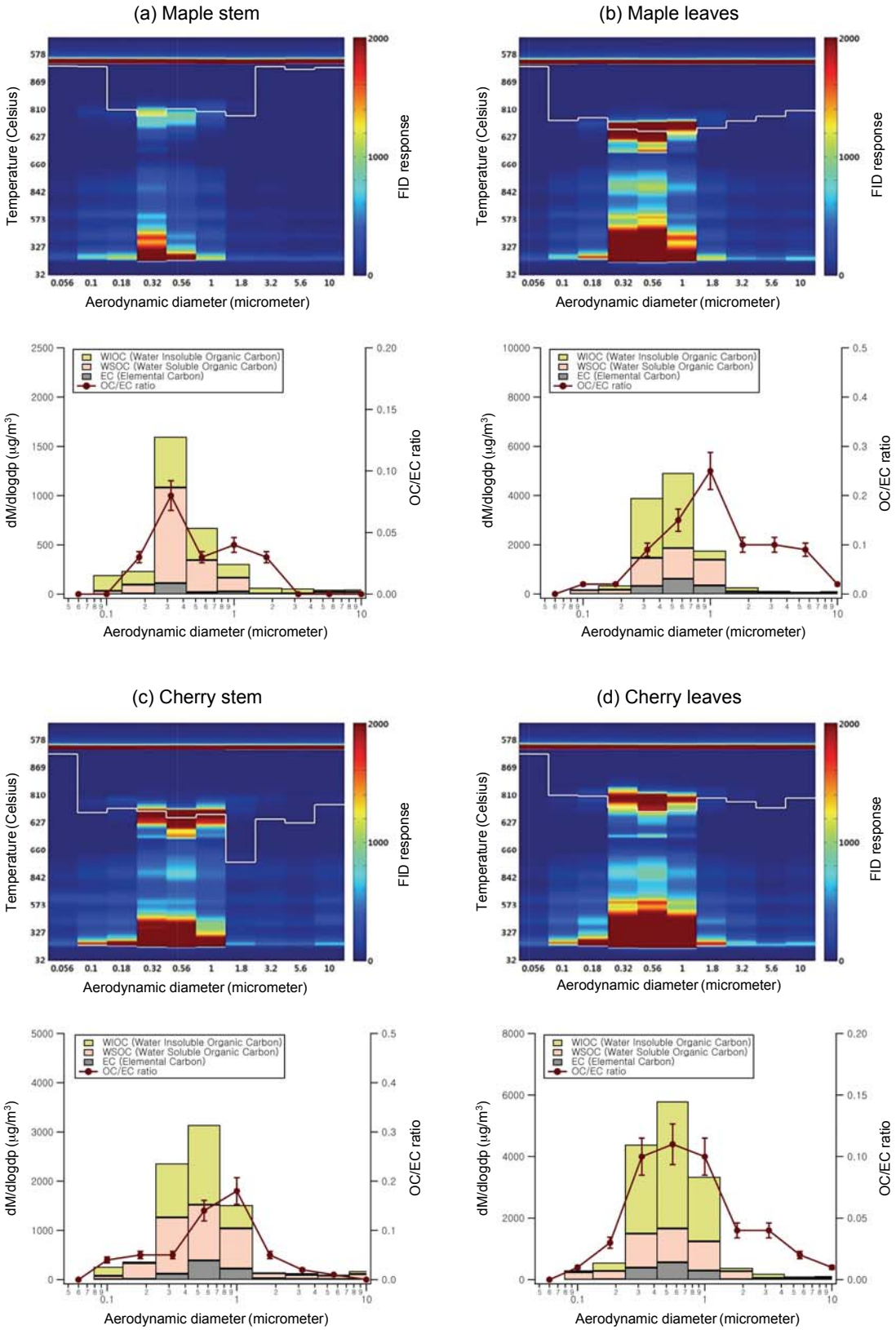

Fig. 4. Sized resolved CTD (top), size distribution of WIOC, WSOC, EC, and OC/EC ratio (bottom) associated with (a) maple stems, (b) maple leaves, (c) cherry stems, and (d) cherry leaves.

concentrations.

3. 3 Maple Stems, Maple Leaves, Cherry Stems, and Cherry Leaves

Fig. 4 illustrates the size-resolved CTD (top), size distribution of WIOC, WSOC, and EC with a size distribution ratio of OC to EC associated with maple stems, maple leaves, cherry stems, and cherry leaves. The CTD patterns for maple leaves, cherry stems, and cherry leaves shown in Fig. 3 are similar except for the maple stems. The peak in maple leaves, cherry stems, and cherry leaves increases to 0.56 μm size while maple stems have a 0.32 μm size. Each biomass size distribution pattern is well correlated between OC and WIOC size distributions (R^2 of 0.96), suggesting that organic compounds in WIOC can contain significant organic tracers for maple and cherry tree contributions to ultrafine aerosol concentrations for a chemical signature to identify source contributions.

4. CONCLUSIONS

Size-resolved carbonaceous distributions have been measured using a MOUDI impactor for four types of agricultural crop residues (rice straw, red pepper stems, soybean stems, and green perilla stems) and eight types of forest tree (pine stems, pine needles, ginkgo stems, ginkgo leaves, maple stems, maple leaves, cherry stems, and cherry leaves) between a 0.056 and 5.6 μm aerosol size. Determination of concentrations of OC, EC, WSOC, and WIOC useful for source apportionment studies are described for each size fraction. Eight types of the forest trees show emission factors of 2.86, 8.20, 2.26, 3.24, 14.32, 1.39, 9.16, and 0.49 for pine stems, pine needles, ginkgo stems, ginkgo leaves, maple stems, maple leaves, cherry stems, and cherry leaves, respectively. The averaged emission factor for the agricultural crop residues is approximately 37% lower than the averaged emission factor for the forest trees.

The CTD patterns for the rice straw, red pepper stems, soybean stems, and green perilla stems can give information about the organic structure such as PAHs related to the biomass burning if the amount of evolved carbon exists at the higher temperature. Similar peaks are observed in the CTD patterns for red pepper stems, soybean stems, and green perilla stems, but not for rice straw. The peak increases to 0.32 μm size while rice straw shows a 0.56 μm size. The cause of this peak may be inferred from the emissions of the different molecular organic marker compounds related to primary combustion. WIOC concentrations had a unimodal size distribution that was highly correlated (R^2 of 0.96) to OC concentrations. The CTD for both ginkgo stem and ginkgo leaves is present at a high temperature ($>800^{\circ}C$) in He. This observation shows that the aromatic compounds that have a higher number of aromatic rings might be related to ginkgo tree combustion. The CTD patterns for maple leaves, cherry stems, and cherry leaves are similar excepting the maple stems. The peak for maple leaves, cherry stems, and cherry leaves increases to 0.56 μm, while the maple stems have a 0.32 μm size. The resolution of source apportionment studies for airborne particulate matter can apparently be increased by the use of WIOC organic tracers that are released only by a well-defined class of burning biomass sources.

ACKNOWLEDGEMENT

We acknowledge the Basic Science Research Program through the National Research Foundation of Korea (NRF) funded by the Ministry of Education, Science and Technology (NRF-2011-0014998) for their support. In addition, we thank Kwang-Yul Lee at Gwangju Institute of Science and Technology (GIST) for help with aerosol sampling.

REFERENCES

Baddock, M.C., Strong, C.L., Murray, P.S., McTainsh, G.H. (2013) Aeolian dust as a transport hazard. Atmospheric Environment 71, 7-14.

Bae, M., Schauer, J.J., DeMinter, J.T., Turner, J.R., Smith, D., Cary, R.A. (2004) Validation of a Semi-Continuous Instrument for Elemental Carbon and Organic Carbon Using a Thermal-Optical Method. Atmospheric Environment 38, 2885-2893.

Bae, M.S., Lee, J.Y., Kim, Y.P., Oak, M.H., Shin, J.S., Lee, K.Y., Lee, H., Lee, S.Y., Kim, Y.J. (2012) Analytical Methods of Levoglucosan, a Tracer for Cellulose in Biomass Burning, by Four Different Techniques. Asian Journal of Atmospheric Environment 6(1), 53-66.

Birch, M. (1998) Analysis of carbonaceous aerosols: interlaboratory comparison. The Analyst 123, 851-857.

Birch, M., Cary, R. (1996) Elemental carbon-based method for monitoring occupational exposures to particulate diesel exhaust. Aerosol Science Technology 25, 221-241.

Chow, J., Watson, J., Chen, L., Chang, M., Robinson, N., Trimble, D., Kohl, S. (2007) The IMPROVE_A temperature protocol for thermal/optical carbon analysis: maintaining consistency with a long-term database. Journal of the Air & Waste Management Association 57, 1014-1023.

Kleeman, M.J., Robert, M.A., Riddle, S.G., Fine, P.M.,

Hays, M.D., Schauer, J.J., Hannigan, M.P. (2008) Size distribution of trace organic species emitted from biomass combustion and meat charbroiling. Atmospheric Environment 42, 3059-3075.

Miller-Schulze, J.P., Shafer, M.M., Schauer, J.J., Solomon, P.A., Lantz, J., Artamonova, M., Chen, B., Imashev, S., Sverdlik, L., Carmichael, G.R., Deminter, J.T. (2011) Characteristics of fine particle carbonaceous aerosol at two remote sites in Central Asia. Atmospheric Environment 45, 6955-6964.

Novakov, T., Corrigan, C. (1996) Cloud condensation nucleus activity of the organic component of biomass smoke particles. Geophys Research Letter 23, 2141-2144.

Park, R.J., Kim, M.J., Jeong, J.I., Youn, D.Y., Kim, S. (2010) A contribution of brown carbon aerosol to the aerosol light absorption and its radiative forcing in East Asia. Atmospheric Environment 44, 1414-1421.

Park, S.S., Sim, S.Y., Bae, M.S., Schauer, J.J. (2013) Size distribution of water-soluble components in particulate matter emitted from biomass burning. Atmospheric Environment 73, 62-72.

Pathak, R.K., Wang, T., Ho, K.F., Lee, S.C. (2011) Characteristics of summertime PM2.5 organic and elemental carbon in four major Chinese cities: Implications of high acidity for water-soluble organic carbon (WSOC). Atmospheric Environment 45, 318-325.

Peralta, O., Baumgardner, D., Raga, G. (2007) Spectrothermography of Carbonaceous particles. Journal of Atmospheric Chemistry 57, 153-169.

Schauer, J.J., Kleeman, M.J., Cass, G.R., Simoneit, B.R.T. (2001) Measurement of Emissions from Air Pollution Sources. 3. C1-C29 Organic Compounds from Fireplace Combustion of Wood. Environmental Science & Technology 35, 1716-1728.

Schneidemesser, E., Zhou, J., Stone, E.A., Schauer, J.J., Qasrawi, R., Abdeen, Z., Shpund, J., Vanger, A., Sharf, G., Moise, T., Brenner, S., Nassar, K., Saleh, R., Al-Mahasneh, Q.M., Sarnat, J.A. (2010) Seasonal and spatial trends in the sources of fine particle organic carbon in Israel, Jordan, and Palestine. Atmospheric Environment 44, 3669-3678.

Smith, K.R. (2000) National burden of disease in India from indoor air pollution. Proceedings of the National Academy of Sciences USA 97, 13286-13293

Sullivan, A.P., Weber, R.J. (2006) Chemical characterization of the ambient organic aerosol soluble in water: 2. isolation of acid, neutral, and basic fractions by modified size-exclusion chromatography. Journal of Geophysical Research 111, D05315. doi:10.1029/2005JD006486.

Thompson, J.E., Hayes, P.L., Jimenez, J.L., Adachi, K., Zhang, X., Liu, J., Weber, R.J., Buseck, P.R. (2012) Aerosol optical properties at Pasadena, CA during CalNex 2010. Atmospheric Environment 55, 190-200.

Vivanco, M.G., Santiago, M., Martínez-Tarifa, A., Borrás, E., Ródenas, M., García-Diego, C., Sánchez, M. (2011) SOA formation in a photoreactor from a mixture of organic gases and HONO for different experimental conditions. Atmospheric Environment 45, 708-715.

Zhang, Y., Sheesley, R.J., Bae, M.S., Schauer, J.J. (2009) Sensitivity of a molecular marker based positive matrix factorization model to the number of receptor observations. Atmospheric Environment 43, 4951-4958.

(Received 17 March 2013, revised 17 May 2013, accepted 28 May 2013)